Available online at www.sciencedirect.com

SciVerse ScienceDirect

Ceramics International 39 (2013) 5527–5533

CERAMICS INTERNATIONAL

www.elsevier.com/locate/ceramint

Electrochemical characteristics of $LiNi_{0.5}Co_{0.5}O_2$ synthesized at 800 °C from the different combinations of carbonates, oxides, and hydroxides

Myoung Youp Song[a,*], Ho Rim[b], Jiunn Song[c], Daniel R. Mumm[d]

[a]*Division of Advanced Materials Engineering, Hydrogen & Fuel Cell Research Center, Engineering Research Institute, Chonbuk National University, 567 Baekje-daero Deokjin-gu Jeonju 561-756, Republic of Korea*

[b]*ASE Korea, 494 Munbal-dong Paju-si Gyeonggi-do 413-790, Republic of Korea*

[c]*College of Arts and Sciences, Cornell University, 147 Goldwin Smith, Ithaca, NY 14853, USA*

[d]*Department of Chemical Engineering and Materials Science, University of California Irvine, Irvine, CA 92697-2575, USA*

Received 10 October 2012; received in revised form 30 November 2012; accepted 19 December 2012
Available online 28 December 2012

Abstract

$LiNi_{0.5}Co_{0.5}O_2$ cathode materials were synthesized by a solid-state reaction method at 800 °C using Li_2CO_3, $LiOH \cdot H_2O$; NiO, $NiCO_3$; $CoCO_3$, or Co_3O_4 as the sources of Li, Ni, and Co, respectively. The electrochemical properties of the synthesized samples were then investigated. The structure of the synthesized $LiNi_{0.5}Co_{0.5}O_2$ was analyzed, and the microstructures of the samples were observed. The curves of voltage vs. x in $Li_xNi_{0.5}Co_{0.5}O_2$ for first charge–discharge and intercalated and deintercalated Li quantity Δx were studied. Destruction of unstable 3b sites and phase transitions were discussed from the first and second charge–discharge curves of voltage vs. x in $Li_xNi_{0.5}Co_{0.5}O_2$. The $LiNi_{0.5}Co_{0.5}O_2$ sample synthesized from Li_2CO_3, $NiCO_3$ and Co_3O_4 has the largest first discharge capacity (142 mAh/g). The $LiNi_{0.5}Co_{0.5}O_2$ sample synthesized from Li_2CO_3, NiO and Co_3O_4 has a relatively large first discharge capacity (141 mAh/g) and the smallest capacity deterioration rate (4.6 mAh/g/cycle).

Keywords: $LiNi_{0.5}Co_{0.5}O_2$; Solid-state reaction method; Various starting materials; Curve of voltage vs. x in $Li_xNi_{0.5}Co_{0.5}O_2$

1. Introduction

$LiCoO_2$ [1–5], $LiNiO_2$ [6–13], and $LiMn_2O_4$ [14–20] have been studied as cathode materials for lithium secondary batteries [21]. $LiMn_2O_4$ is relatively inexpensive and environment-friendly, but its cycling performance is poor. $LiCoO_2$ has a large diffusivity and a high operating voltage, and its synthesis is easy. However, it has a disadvantage that it contains an expensive element, Co.

$LiNiO_2$ has a large discharge capacity [22] and is relatively excellent economically and environmentally. However, since Li and Ni have similar sizes ($Li^+ = 0.72$ Å and $Ni^{2+} = 0.69$ Å), the $LiNiO_2$ is practically obtained in the non-stoichiometric compositions, $Li_{1-y}Ni_{1+y}O_2$ [23,24]. The Ni^{2+} ions in the lithium planes obstruct the movement of the Li^+ ions during intercalation and deintercalation [25,26].

To overcome the shortcomings of $LiCoO_2$ and $LiNiO_2$, $LiCoO_2$ and $LiNiO_2$ phases were incorporated into $LiNi_{1-y}Co_yO_2$ compositions because the presence of cobalt stabilizes the structure in a strictly two-dimensional fashion, thus favoring good reversibility of the intercalation and deintercalation reactions [25,27–39]. Rougier et al. [25] reported that the stabilization of the two-dimensional character of the structure by cobalt substitution in $LiNiO_2$ is correlated with an increase in cell performance, due to the decrease in the amount of extra-nickel ions in the inter-slab space which impede the lithium diffusion. Kang et al. [39] investigated the structure and electrochemical properties of the $Li_xCo_yNi_{1-y}O_2$ ($y = 0.1$, 0.3, 0.5, 0.7 and 1.0) system synthesized by the solid state reaction with various starting materials to optimize the characteristics and synthetic conditions of the $Li_xCo_yNi_{1-y}O_2$.

*Corresponding author. Tel.: +82 63 270 2379; fax: +82 63 270 2386.
E-mail address: songmy@jbnu.ac.kr (M. Youp Song).

0272-8842/$ - see front matter © 2012 Elsevier Ltd and Techna Group S.r.l. All rights reserved.
http://dx.doi.org/10.1016/j.ceramint.2012.12.066

The first discharge capacities of $Li_xCo_yNi_{1-y}O_2$ were 60–180 mAh/g depending on synthesis conditions.

Several methods to synthesize $LiNiO_2$ and $LiNi_{1-y}Co_yO_2$ are reported, such as solid-state reaction method [40,41], coprecipitation method [42], sol–gel method [43], ultrasonic spray pyrolysis method [44], combustion method [11], and emulsion method [45]. In this work, the solid state reaction method, which is quite simple, was used.

Different starting materials are employed by researchers to synthesize $LiNi_{1-y}Co_yO_2$ by the solid-state reaction method [25,27–30,32–34,38,39,46]. $LiOH \cdot H_2O$ or Li_2CO_3, NiO or $NiCO_3$, and Co_3O_4 or $CoCO_3$ have been used as starting materials by some researchers [39,46] in order to synthesize $LiNi_{1-y}Co_yO_2$ by the solid-state reaction method.

In this work, $LiNi_{0.5}Co_{0.5}O_2$ cathode materials were synthesized by a solid-state reaction method at 800 °C using Li_2CO_3, $LiOH \cdot H_2O$; NiO, $NiCO_3$; $CoCO_3$, or Co_3O_4 as the sources of Li, Ni, and Co, respectively. The electrochemical properties of the synthesized samples were then investigated. The structure of the synthesized $LiNi_{0.5}Co_{0.5}O_2$ was analyzed, and the microstructures of the samples were observed. The curves of voltage vs. x in $Li_xNi_{0.5}Co_{0.5}O_2$ for first charge–discharge and intercalated and deintercalated Li quantity Δx were studied. Destruction of unstable 3b sites and phase transitions were discussed from the first and second charge–discharge curves of voltage vs. x in $Li_xNi_{0.5}Co_{0.5}O_2$.

2. Experimental

Li_2CO_3, $LiOH \cdot H_2O$, NiO, $NiCO_3$, $CoCO_3$, or Co_3O_4 were used as starting materials in order to synthesize $LiNi_{0.5}Co_{0.5}O_2$ by the solid-state reaction method. All the starting materials (with the purity of 99.9%) were purchased from Aldrich Co.

The experimental procedure for the synthesis of $LiNi_{0.5}Co_{0.5}O_2$ from Li_2CO_3, $LiOH \cdot H_2O$, NiO, $NiCO_3$, $CoCO_3$, or Co_3O_4 and the characterization of the synthesized samples is given schematically in Fig. 1. The mixture of the starting materials with the composition of $LiNi_{0.5}Co_{0.5}O_2$ was sufficiently mixed and pelletized. The pellet was then heat-treated in air at 650 °C for 20 h. It was then ground, mixed, pelletized, and calcined at 800 °C for 20 h. Then, this pellet was cooled at a cooling rate of 50 °C/min, ground, mixed, and pelletized again. Finally, it was calcined again at 800 °C for 20 h.

The phase identification of the synthesized samples was carried out by X-ray diffraction (XRD) analysis using Cu K_α radiation (Mac-Science Co., Ltd.). The scanning rate was 16°/min and the scanning range of diffraction angle (2θ) is $10° \le 2\theta \le 70°$. The morphologies of the samples were observed using a scanning electron microscope (SEM).

The electrochemical cells consisted of $LiNi_{0.5}Co_{0.5}O_2$ as a positive electrode, Li foil as a negative electrode, and electrolyte of 1 M $LiPF_6$ in a 1: 1 (volume ratio) mixture of ethylene carbonate (EC) and dimethyl carbonate (DMC).

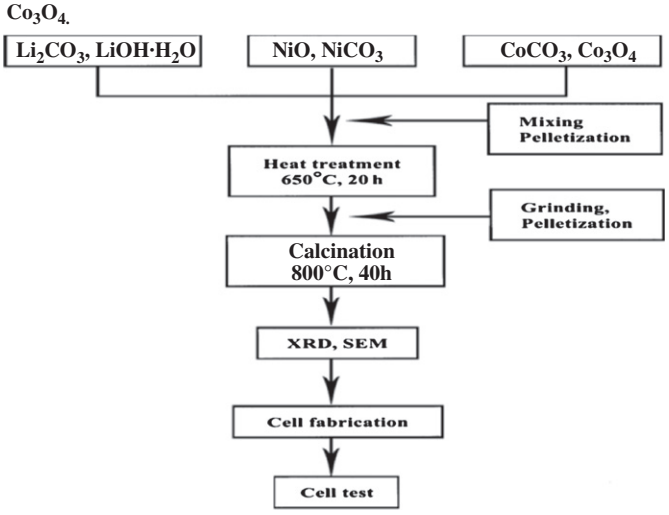

Fig. 1. Experimental procedure for $LiNi_{0.5}Co_{0.5}O_2$ synthesis from Li_2CO_3, $LiOH \cdot H_2O$, NiO, $NiCO_3$, $CoCO_3$, or Co_3O_4 and characterization of the synthesized $LiNi_{0.5}Co_{0.5}O_2$.

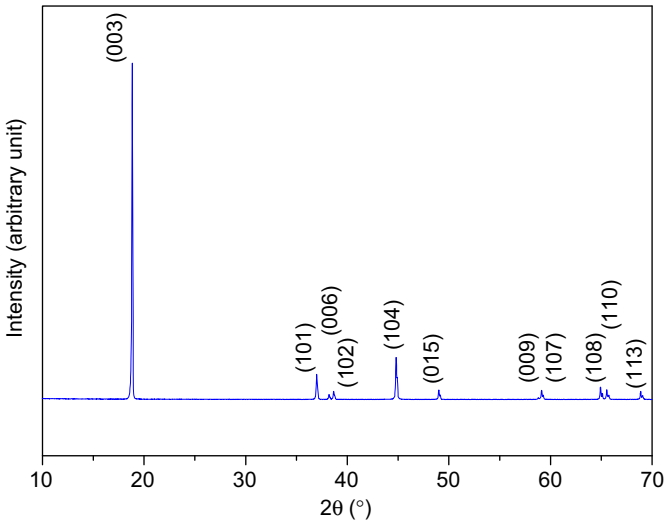

Fig. 2. XRD pattern of $LiNi_{0.5}Co_{0.5}O_2$ powder calcined at 800 °C for 40 h using Li_2CO_3, $NiCO_3$ and Co_3O_4 as starting materials.

A Whatman glass-fiber was used as the separator. The cells were assembled in an argon-filled dry box. To fabricate the positive electrode, 89 wt% synthesized oxide, 10 wt% acetylene black, and 1 wt% polytetrafluoroethylene (PTFE) binder were mixed in an agate mortar. By introducing Li metal, Whatman glass-fiber, positive electrode, and the electrolyte, the cell was assembled. All the electrochemical tests were performed at room temperature with a potentiostatic/galvanostatic system (Mac-Pile system, Bio-Logic Co. Ltd.). The cells were cycled at a current density of 200 μA/cm^2 in a voltage range of 3.2–4.3 V.

3. Results and discussion

The XRD pattern of $LiNi_{0.5}Co_{0.5}O_2$ powder calcined at 800 °C for 40 h using Li_2CO_3, $NiCO_3$ and Co_3O_4 as

starting materials is shown in Fig. 2. The peaks are identified as corresponding to those of the $LiNiO_2$ phase, which has α-$NaFeO_2$ structure with a space group of $R\bar{3}m$. The fraction of each phase from the intensity ratios of the 003 and 104 peaks can be calculated since the 003 peak originates from the diffraction of only $R\bar{3}m$ α-$NaFeO_2$ structure while the 104 peak originates from the diffractions of both $R\bar{3}m$ α-$NaFeO_2$ and $Fm\bar{3}m$ NaCl structures. The intensity ratio of the 003 and 104 peaks, I_{003}/I_{104}, of the completely stoichiometric composition $LiNiO_2$ was reported to be about 1.3 by Morales et al. [24]. Ohzuku et al. [40] reported that the intensity ratio of 003 and 104 peaks is a key parameter of the degree of displacement of the nickel and lithium ions. As the intensity ratio of 003 and 104 peaks increases, the degree of displacement of the nickel and lithium ions decreases. They also reported that electroactive $LiNiO_2$ showed a clear split of (108) and (110) lines, which appear in their XRD patterns at a diffraction angle near $2\theta=65^\circ$.

Fig. 3 shows the SEM micrographs of $LiNi_{0.5}Co_{0.5}O_2$ synthesized at 800 °C from the combination of starting materials: (a) Li_2CO_3, NiO and $CoCO_3$, (b) $LiOH \cdot H_2O$, NiO and Co_3O_4, (c) Li_2CO_3, NiO and Co_3O_4, (d) Li_2CO_3, $NiCO_3$ and Co_3O_4, and (e) Li_2CO_3, $NiCO_3$ and $CoCO_3$. The samples (a), (b), and (c) have small and large particles with flat surfaces. Among these three samples, the sample (b) has the largest particles, and the samples (b) and (c) have similar particle sizes. The sample (c) has small particles with spherical shape. The sample (d) has large spherical particles. Over all, the sample (d) has the largest particles, followed in order by the sample (b), the sample (c), the sample (a), and the sample (d).

The voltage vs. x in $Li_xNi_{0.5}Co_{0.5}O_2$ curves at a current density of 200 μA/cm^2 for the first charge–discharge of $LiNi_{0.5}Co_{0.5}O_2$ synthesized at 800 °C from the combination of starting materials: (a) Li_2CO_3, NiO and $CoCO_3$, (b) $LiOH \cdot H_2O$, NiO and Co_3O_4, (c) Li_2CO_3, NiO and Co_3O_4, (d) Li_2CO_3, $NiCO_3$ and Co_3O_4, and (e) Li_2CO_3, $NiCO_3$ and $CoCO_3$ are shown in Fig. 4. Polarization is a change in the potentials for deintercalation and intercalation of lithium atoms. The samples (e), (b) and (d) have smaller polarization than the samples (a) and (c). The differences

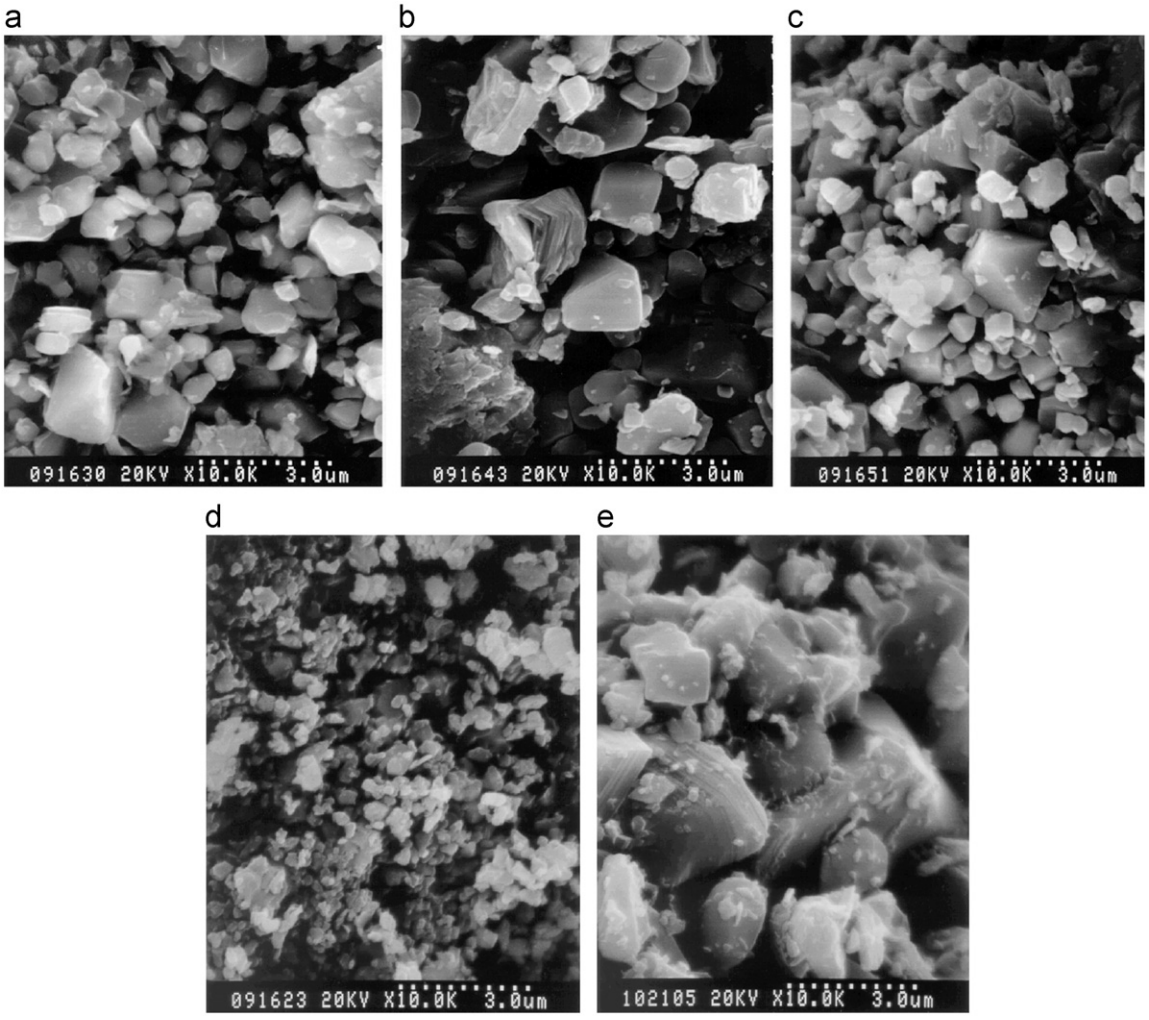

Fig. 3. SEM micrographs of the $LiNi_{0.5}Co_{0.5}O_2$ synthesized at 800 °C from the combinations of starting materials: (a) Li_2CO_3, NiO and $CoCO_3$, (b) $LiOH \cdot H_2O$, NiO and Co_3O_4, (c) Li_2CO_3, NiO and Co_3O_4, (d) Li_2CO_3, $NiCO_3$ and Co_3O_4, and (e) Li_2CO_3, $NiCO_3$ and $CoCO_3$.

in x between the first charge and the first discharge of the samples (a) and (c) are larger than those of the samples (e), (b) and (d). This shows that the structures of the samples (a) and (c) are more unstable than those of the samples (e), (b) and (d) and thus during the first charge–discharge cycle the Li sites are destroyed. The intensity ratio, I_{003}/I_{104}, of 003 and 104 peaks in XRD pattern is known as an indicator for cation mixing. The sample with a larger value of I_{003}/I_{104} has a smaller cation mixing. The I_{003}/I_{104} value of the sample (c) (1.410) is smaller than that of the sample (b) (1.477). A low "crystallinity index", I_{max}/B, from the XRD pattern of a sample indicates a low crystallinity of the sample. I_{max} is the maximum height of a peak and B is the full width at half maximum of the peak. The sample (c) (2.387) has a smaller I_{max}/B value than the sample (b) (3.620), indicating that the sample (c) has a poorer crystallinity than the sample (b). It is believed that the more unstable Li sites of the samples (a) and (c) led to the larger polarization of the samples (a) and (c) than that of the samples (e), (b) and (d). In addition, the larger cation mixing, and the poorer crystallinity of the sample (c) than the sample (b) led to the larger polarization of the sample (c) than that of the sample (b).

The charge or discharge capacity is proportional to the value of Δx in $Li_xNi_{0.5}Co_{0.5}O_2$. The sample (d) has the largest discharge capacity, followed in order by the sample (c), the sample (b), the sample (e), and the sample (a).

Fig. 5 shows the voltage vs. x in $Li_xNi_{0.5}Co_{0.5}O_2$ curves for the first and second charge–discharge cycles for $LiNi_{0.5}Co_{0.5}O_2$ synthesized at 800 °C from Li_2CO_3, $NiCO_3$ and $CoCO_3$. The value of Δx for the second discharge is slightly smaller than that for the first discharge.

The variations of the discharge capacity with the number of cycles (n) for $LiNi_{0.5}Co_{0.5}O_2$ synthesized at 800 °C from (a) Li_2CO_3, NiO and $CoCO_3$, (b) $LiOH \cdot H_2O$, NiO and Co_3O_4, (c) Li_2CO_3, NiO and Co_3O_4, (d) Li_2CO_3, $NiCO_3$ and Co_3O_4, and (e) Li_2CO_3, $NiCO_3$ and $CoCO_3$ are shown in Fig. 6. The sample (d) has the largest first discharge capacity, followed in order by the sample (c), the sample (b), the sample (e), and the sample (a). The samples (b), (c), and (d) have similar and relatively good cycling performances.

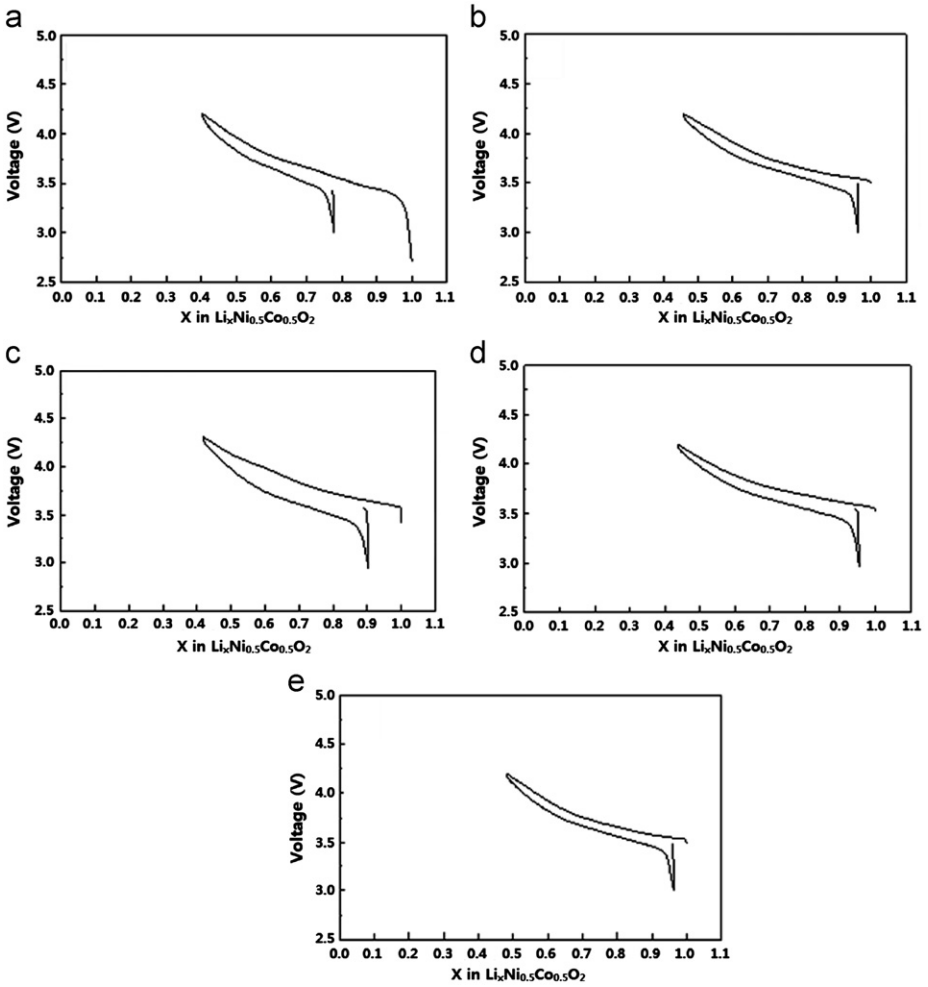

Fig. 4. Voltage vs. x in $Li_xNi_{0.5}Co_{0.5}O_2$ curves at a current density of 200 μA/cm^2 for the first charge–discharge of $LiNi_{0.5}Co_{0.5}O_2$ synthesized at 800 °C from the combinations of starting materials: (a) Li_2CO_3, NiO and $CoCO_3$, (b) $LiOH \cdot H_2O$, NiO and Co_3O_4, (c) Li_2CO_3, NiO and Co_3O_4, (d) Li_2CO_3, $NiCO_3$ and Co_3O_4, and (e) Li_2CO_3, $NiCO_3$ and $CoCO_3$.

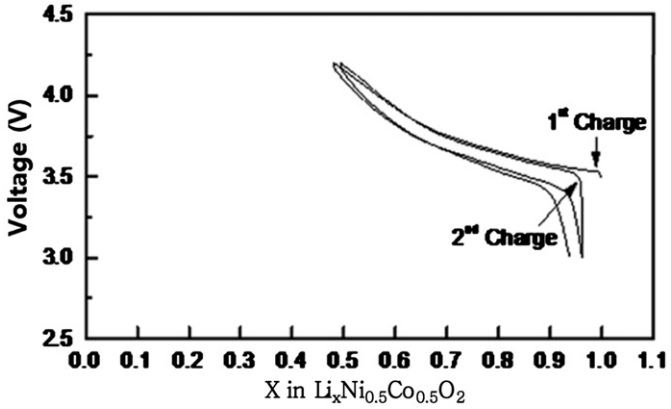

Fig. 5. Voltage vs. x in $Li_xNi_{0.5}Co_{0.5}O_2$ curves for the first and second charge–discharge cycles for $LiNi_{0.5}Co_{0.5}O_2$ synthesized at 800 °C from Li_2CO_3, $NiCO_3$ and $CoCO_3$.

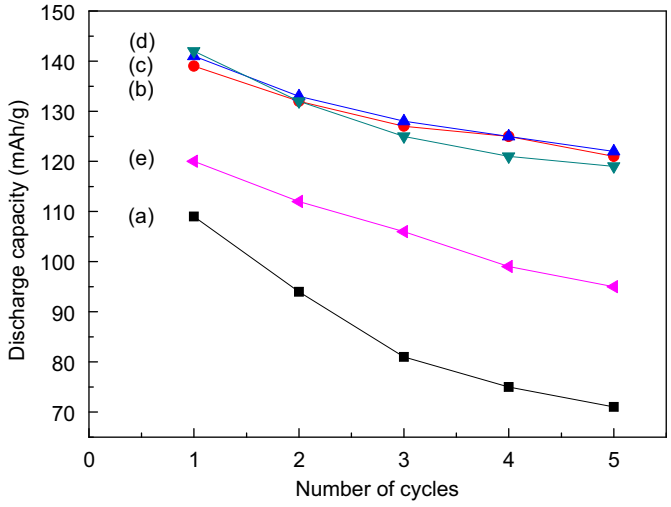

Fig. 6. Variations of the discharge capacity with number of cycles (n) for $LiNi_{0.5}Co_{0.5}O_2$ synthesized at 800 °C from (a) Li_2CO_3, NiO and $CoCO_3$, (b) $LiOH \cdot H_2O$, NiO and Co_3O_4, (c) Li_2CO_3, NiO and Co_3O_4, (d) Li_2CO_3, $NiCO_3$ and Co_3O_4, and (e) Li_2CO_3, $NiCO_3$ and $CoCO_3$.

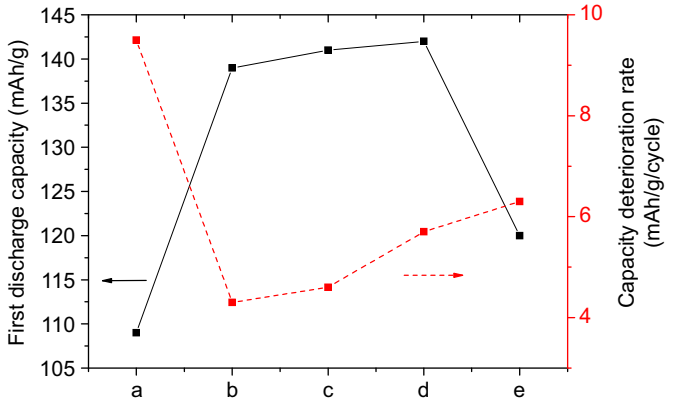

Fig. 7. Variations of the first discharge capacity and the capacity deterioration rate of $LiNi_{0.5}Co_{0.5}O_2$ synthesized at 800 °C with the combination of starting materials: (a) Li_2CO_3, NiO and $CoCO_3$, (b) $LiOH \cdot H_2O$, NiO and Co_3O_4, (c) Li_2CO_3, NiO and Co_3O_4, (d) Li_2CO_3, $NiCO_3$ and Co_3O_4, and (e) Li_2CO_3, $NiCO_3$ and $CoCO_3$.

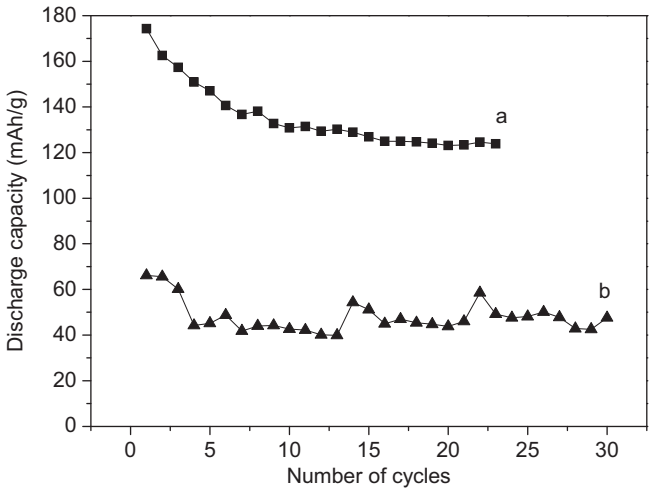

Fig. 8. Variations of the discharge capacity at 200 μA/cm^2 with the number of cycles for $LiNi_{0.5}Co_{0.5}O_2$ calcined for 40 h (a) at 800 °C and (b) at 750 °C from $LiOH \cdot H_2O$, NiO and Co_3O_4.

Fig. 7 shows the variations of the first discharge capacity and the capacity deterioration rate of $LiNi_{0.5}Co_{0.5}O_2$ synthesized at 800 °C with the combination of starting materials: (a) Li_2CO_3, NiO and $CoCO_3$, (b) $LiOH \cdot H_2O$, NiO and Co_3O_4, (c) Li_2CO_3, NiO and Co_3O_4, (d) Li_2CO_3, $NiCO_3$ and Co_3O_4, and (e) Li_2CO_3, $NiCO_3$ and $CoCO_3$. The sample (d) has the largest first discharge capacity (142 mAh/g), followed in order by the sample (c) (141 mAh/g), the sample (b) (139 mAh/g), the sample (e) (120 mAh/g), and the sample (a) (109 mAh/g). The sample (b) has the smallest capacity deterioration rate (4.3 mAh/g/cycle), followed in order by the sample (c) (4.6 mAh/g/cycle), the sample (d) (5.7 mAh/g/cycle), the sample (e) (6.3 mAh/g/cycle), and the sample (a) (9.5 mAh/g/cycle).

The variations of the discharge capacity at 200 μA/cm^2 with the number of cycles for $LiNi_{0.5}Co_{0.5}O_2$ calcined for 40 h at (a) 800 °C for 23 cycles and (b) 750 °C for 30 cycles from $LiOH \cdot H_2O$, NiO and Co_3O_4 are shown in Fig. 8. The $LiNi_{0.5}Co_{0.5}O_2$ calcined at 800 °C has larger discharge capacities than that calcined at 750 °C. $LiNi_{0.5}Co_{0.5}O_2$ calcined at 800 °C shows almost constant discharge capacity from about 10th cycle. It has discharge capacities of 174.3, 130.8 and 123.8 mAh/g at $n=1$, $n=10$ and $n=23$, respectively. The $LiNi_{0.5}Co_{0.5}O_2$ calcined at 750 °C shows almost constant discharge capacity from about fifth cycle, its discharge capacity fluctuating with the number of cycles. These results show that the discharge capacities remain nearly constant after $n=5$–10.

The curves of the voltage vs. x in $Li_xNi_{0.5}Co_{0.5}O_2$ at a current density of 200 μA/cm^2 for the first charge–discharge of $LiNi_{0.5}Co_{0.5}O_2$ in Fig. 4 show that, as compared with the quantity of the deintercalated Li ions by the first charging, with that of the intercalated Li ions by the first discharging is much smaller, which is revealed

by the difference in Δx of the first charge and discharge curves, for this sample. The lengths of plateaus in the charge and discharge curves are proportional to charge and discharge capacities. During the first charging, Li ions deintercalate not only from stable 3b sites but also from unstable 3b sites. After deintercalation from unstable 3b sites, the unstable 3b sites will be destroyed. This is considered to lead to smaller quantity of the intercalated Li ions by the first discharging than that of the deintercalated Li ions by the first charging.

The curves of the voltage vs. x in $Li_xNi_{0.5}Co_{0.5}O_2$ for the first and second charge–discharge of $LiNi_{0.5}Co_{0.5}O_2$ synthesized at 800 °C in Fig. 5 show that the difference in Δx of the second charge and discharge curves is smaller than that of the first charge and discharge curves. This shows that the destruction of unstable 3b sites occurs less severely at the second cycle than at the first cycle.

In the curves of the voltage vs. x in $Li_xNi_{0.5}Co_{0.5}O_2$ for the first and second charge–discharge of $LiNi_{0.5}Co_{0.5}O_2$ synthesized at 800 °C in Fig. 5, the charge–discharge curves exhibit quite long plateaus, where two phases coexist [47]. Arai et al. [48] reported that, during charging and discharging, $LiNiO_2$ goes through three phase transitions; phase transitions from hexagonal structure (H1) to monoclinic structure (M), from monoclinic structure (M) to hexagonal structure (H2), and from hexagonal structure (H2) to hexagonal structure (H3) or vice versa. Ohzuku et al. [40] reported that, during charging and discharging, $LiNiO_2$ goes through four phase transitions; phase transitions from H1 to M, from M to H2, from H2 to hexagonal structures H2+H3, and from H2+H3 to H3 or vice versa. Song et al. [49] reported that $-dx/|dV|$ vs. V curves of $LiNi_{1-y}Ti_yO_2$ ($y=0.012$ and 0.025) for charging and discharging showed four peaks, revealing the four phase transitions from H1 to M, from M to H2, from H2 to H2+H3, and from H2+H3 to H3 or vice versa.

4. Conclusions

$LiNi_{0.5}Co_{0.5}O_2$ cathode materials were synthesized by a solid-state reaction method at 800 °C using Li_2CO_3, $LiOH \cdot H_2O$; NiO, $NiCO_3$; $CoCO_3$, or Co_3O_4 as the sources of Li, Ni, and Co, respectively. The electrochemical properties of the synthesized samples were then investigated. The $LiNi_{0.5}Co_{0.5}O_2$ sample synthesized from Li_2CO_3, $NiCO_3$ and Co_3O_4 has the largest first discharge capacity (142 mAh/g). The $LiNi_{0.5}Co_{0.5}O_2$ sample synthesized from Li_2CO_3, NiO and Co_3O_4 has the relatively large first discharge capacity (141 mAh/g) and the smallest capacity deterioration rate (4.6 mAh/g/cycle). The curves of the voltage vs. x in $Li_xNi_{0.5}Co_{0.5}O_2$ for the first charge–discharge of $LiNi_{0.5}Co_{0.5}O_2$ showed that after deintercalation from unstable 3b sites, the unstable 3b sites will be destroyed, leading to a smaller quantity of the intercalated Li ions by the first discharging than that of the deintercalated Li ions by the first charging.

References

[1] K. Ozawa, Lithium-ion rechargeable batteries with $LiCoO_2$ and carbon electrodes: the $LiCoO_2$/C system, Solid State Ionics 69 (1994) 212–221.

[2] R. Alcántara, P. Lavela, J.L. Tirado, R. Stoyanova, E. Zhecheva, Structure and electrochemical properties of boron-doped $LiCoO_2$, Journal of Solid State Chemistry 134 (1997) 265–273.

[3] Z.S. Peng, C.R. Wan, C.Y. Jiang, Synthesis by sol–gel process and characterization of $LiCoO_2$ cathode materials, Journal of Power Sources 72 (1998) 215–220.

[4] W.D. Yang, C.Y. Hsieh, H.J. Chuang, Y.S. Chen, Preparation and characterization of nanometric-sized $LiCoO_2$ cathode materials for lithium batteries by a novel sol–gel method, Ceramics International 36 (1) (2010) 135–140.

[5] S.K. Kim, D.H. Yang, J.S. Sohn, Y.C. Jung, Resynthesis of $LiCo_{1-x}Mn_xO_2$ as a cathode material for lithium secondary batteries, Metals and Materials International 18 (2) (2012) 321–326.

[6] J.R. Dahn, U. von Sacken, C.A. Michal, Structure and electrochemistry of $Li_{1\pm y}NiO_2$ and a new Li_2NiO_2 phase with the $Ni(OH)_2$ structure, Solid State Ionics 44 (1990) 87–97.

[7] J.R. Dahn, U. von Sacken, M.W. Juzkow, H. Al-Janaby, Rechargeable $LiNiO_2$/carbon cells, Journal of the Electrochemical Society 138 (1991) 2207–2212.

[8] H.U. Kim, D.R. Mumm, H.R. Park, M.Y. Song, Synthesis by a simple combustion method and electrochemical properties of Li $Co_{1/3}Ni_{1/3}Mn_{1/3}O_2$, Electronic Materials Letters 6 (3) (2010) 91–95.

[9] S.H. Ju, J.H. Kim, Y.C. Kang, Electrochemical properties of $LiNi_{0.8}Co_{0.2-x}Al_xO_2$ ($0 \le x \le 0.1$) cathode particles prepared by spray pyrolysis from the spray solutions with and without organic additives, Metals and Materials International 16 (2) (2010) 299–303.

[10] D.H. Kim, Y.U. Jeong, D.H. Kim, Y.U. Jeong, Crystal structures and electrochemical properties of $LiNi_{1-x}Mg_xO_2$ ($0 \le x \le 0.1$) for cathode materials of secondary lithium batteries, Korean Journal of Metals and Materials 48 (3) (2010) 262–267.

[11] S.N. Kwon, J.H. Song, D.R. Mumm, Effects of cathode fabrication conditions and cycling on the electrochemical performance of $LiNiO_2$ synthesized by combustion and calcination, Ceramics International 37 (5) (2011) 1543–1548.

[12] M.Y. Song, C.K. Park, H.R. Park, D.R. Mumm, Variations in the electrochemical properties of metallic elements-substituted $LiNiO_2$ cathodes with preparation and cathode fabrication conditions, Electronic Materials Letters 8 (1) (2012) 37–42.

[13] M.Y. Song, D.R. Mumm, C.K. Park, H.R. Park, Cycling performances of $LiNi_{1-y}M_yO_2$ (M=Ni, Ga, Al and/or Ti) synthesized by wet milling and solid-state method, Metals and Materials International 18 (3) (2012) 465–472.

[14] J.M. Tarascon, E. Wang, F.K. Shokoohi, W.R. Mckinnon, S. Colson, The spinel phase of $LiMn_2O_4$ as a cathode in secondary lithium cells, Journal of the Electrochemical Society 138 (1991) 2859–2864.

[15] A.R. Armstrong, P.G. Bruce, Synthesis of layered $LiMnO_2$ as an electrode for rechargeable lithium batteries, Nature Letters 381 (1996) 499–500.

[16] M.Y. Song, D.S. Ahn, On the capacity deterioration of spinel phase $LiMn_2O_4$ with cycling around 4 V, Solid State Ionics 112 (1998) 21–24.

[17] M.Y. Song, D.S. Ahn, H.R. Park, Capacity fading of spinel phase $LiMn_2O_4$ with cycling, Journal of Power Sources 83 (1999) 57–60.

[18] D.S. Ahn, M.Y. Song, Variations of the electrochemica properties of $LiMn_2O_4$ with synthesis conditions, Journal of the Electrochemical Society 147 (3) (2000) 874–879.

[19] H.J. Guo, Q.H. Li, X.H. Li, Z.X. Wang, W.J. Peng, Novel synthesis of $LiMn_2O_4$ with large tap density by oxidation of manganese powder, Energy Conversion and Management 52 (4) (2011) 2009–2014.

[20] C. Wan, M. Cheng, D. Wu, Synthesis of spherical spinel $LiMn_2O_4$ with commercial manganese carbonate, Powder Technology 210 (1) (2011) 47–51.

[21] J.W. Park, J.H. Yu, K.W. Kim, H.S. Ryu, J.H. Ahn, C.S. Jin, K.H. Shin, Y.C. Kim, H.J. Ahn, Surface morphology changes of lithium/sulfur battery using multi-walled carbon nanotube added sulfur electrode during cyclings, Korean Journal of Metals and Materials 49 (2) (2011) 174–179.
[22] Y. Nishida, K. Nakane, T. Satoh, Synthesis and properties of gallium-doped $LiNiO_2$ as the cathode material for lithium secondary batteries, Journal of Power Sources 68 (1997) 561–564.
[23] P. Barboux, J.M. Tarascon, F.K. Shokoohi, The use of acetates as precursors for the low-temperature synthesis of $LiMn_2O_4$ and $LiCoO_2$ intercalation compounds, Journal of Solid State Chemistry 94 (1991) 185–196.
[24] J. Morales, C. Perez-Vicente, J.L. Tirado, Cation distribution and chemical deintercalation of $Li_{1-x}Ni_{1+x}O_2$, Materials Research Bulletin 25 (1990) 623–630.
[25] A. Rougier, I. Saadoune, P. Gravereau, P. Willmann, C. Delmas, Effect of cobalt substitution on cationic distribution in $LiNi_{1-y}Co_yO_2$ electrode materials, Solid State Ionics 90 (1996) 83–90.
[26] B.J. Neudecker, R.A. Zuhr, B.S. Kwak, J.B. Bates, J.D. Robertson, Lithium manganese nickel oxides $Li_x(Mn_yNi_{1-y})_{2-x}O_2$, Journal of the Electrochemical Society 145 (1998) 4148–4157.
[27] C. Delmas, I. Saadoune, Electrochemical and physical properties of the $Li_xNi_{1-y}Co_yO_2$ phases, Solid State Ionics 53–56 (1992) 370–375.
[28] E. Zhecheva, R. Stoyanova, Stabilization of the layered crystal structure of $LiNiO_2$ by Co-substitution, Solid State Ionics 66 (1993) 143–149.
[29] C. Delmas, I. Saadoune, A. Rougier, The cycling properties of the $Li_xNi_{1-y}Co_yO_2$ electrode, Journal of Power Sources 43–44 (1993) 595–602.
[30] A. Ueda, T. Ohzuku, Solid-state redox reactions of $LiNi_{1/2}Co_{1/2}O_2$ ($R\bar{3}m$) for 4 V secondary lithium cells, Journal of the Electrochemical Society 141 (1994) 2010–2014.
[31] M. Menetrier, A. Rougier, C. Delmas, Cobalt segregation in the $LiNi_{1-y}Co_yO_2$ solid solution: a preliminary ^7Li NMR study, Solid State Communications 90 (1994) 439–442.
[32] R. Alcantara, J. Morales, J.L. Tirado, R. Stoyanova, E. Zhecheva, Structure and electrochemical properties of $Li_{1-x}(Ni_yCo_{1-y})_{1+x}O_2$ Effect of chemical delithiation at 0 °C, Journal of the Electrochemical Society 142 (1995) 3997–4005.
[33] B. Banov, J. Bourilkov, M. Mladenov, Cobalt stabilized layered lithium–nickel oxides, cathodes in lithium rechargeable cells, Journal of Power Sources 54 (1995) 268–270.
[34] Y.M. Choi, S.I. Pyun, S.I. Moon, Effects of cation mixing on the electrochemical lithium intercalation reaction into porous $Li_{1-\delta}Ni_{1-y}Co_yO_2$ electrodes, Solid State Ionics 89 (1996) 43–52.
[35] S.J. Lee, J.K. Lee, D.W. Kim, H.K. Baik, S.M. Lee, Fabrication of thin film $LiCo_{0.5}Ni_{0.5}O_2$ cathode for Li rechargeable microbattery, Journal of the Electrochemical Society 143 (1996) L268–L270.
[36] D. Caurant, N. Baffier, B. Garcia, J.P. Pereira-Ramos, Synthesis by a soft chemistry route and characterization of $LiNi_xCo_{1-x}O_2$ ($0 \le x \le 1$) cathode materials, Solid State Ionics 91 (1996) 45–54.
[37] K. Amine, H. Yasuda, Y. Fujita, New process for low temperature preparation of $LiNi_{1-x}Co_xO_2$ Cathode material for lithium cells, Annales de Chimie—Science des Matériaux 23 (1998) 37–42.
[38] C.C. Chang, N. Scarr, P.N. Kumta, Synthesis and electrochemical characterization of $LiMO_2$ (M=Ni, $Ni_{0.75}Co_{0.25}$) for rechargeable lithium ion batteries, Solid State Ionics 112 (1998) 329–344.
[39] S.G. Kang, K.S. Ryu, S.H. Chang, S.C. Park, The novel synthetic route to $LiCo_yNi_{1-y}O_2$ as a cathode material in lithium secondary batteries, Bulletin of the Korean Chemical Society 22 (12) (2001) 1328–1332.
[40] T. Ohzuku, A. Ueda, M. Nagayama, Electrochemistry and structural chemistry of $LiNiO_2$ ($R\bar{3}m$) for 4 V secondary lithium cells, Journal of the Electrochemical Society 140 (1993) 1862–1870.
[41] Z. Lu, X. Huang, H. Haung, L. Chen, J. Schoonman, The phase transition and optimal synthesis temperature of $LiNiO_2$, Solid State Ionics 120 (1999) 103–107.
[42] M. Guilmard, A. Rougier, M. Grune, L. Croguennec, C. Delmas, Effects of aluminum on the structural and electrochemical properties of $LiNiO_2$, Journal of Power Sources 115 (2003) 305–314.
[43] B.J. Hwang, R. Santhanam, C.H. Chen, Effect of synthesis conditions on electrochemical properties of $LiCo_yNi_{1-y}O_2$ cathode for lithium rechargeable batteries, Journal of Power Sources 114 (2003) 244–252.
[44] S.H. Park, C.S. Yoon, S.G. Kang, H.S. Kim, S.I. Moon, Y.K. Sun, Synthesis and structural characterization of layered Li $[Ni_{1/3}Co_{1/3}Mn_{1/3}]O_2$ cathode materials by ultrasonic spray pyrolysis method, Electrochimica Acta 49 (2004) 557–563.
[45] B.H. Kim, J.H. Kim, I.H. Kwon, M.Y. Song, Electrochemical properties of $LiNiO_2$ cathode material synthesized by the emulsion method, Ceramics International 33 (2007) 837–841.
[46] M.Y. Song, H. Rim, E. Bang, Electrochemical properties of cathode materials $LiNi_{1-y}Co_yO_2$ synthesized using various starting materials, Journal of Applied Electrochemistry 34 (2004) 383–389.
[47] W. Li, J.N. Reimers, J.R. Dahn, In situ X-ray diffraction and electrochemical studies of $Li_{1-x}NiO_2$, Solid State Ionics 67 (1993) 123–130.
[48] H. Arai, S. Okada, H. Ohtsuka, M. Ichimura, J. Yamaki, Characterization and cathode performance of $Li_{1-x}Ni_{1+x}O_2$ prepared with the excess lithium method, Solid State Ionics 80 (1995) 261–269.
[49] M.Y. Song, D.S. Lee, H.R. Park, Electrochemical properties of $LiNi_{1-y}Ti_yO_2$ and $LiNi_{0.975}M_{0.025}O_2$ (M=Zn, Al, and Ti) synthesized by the solid-state reaction method, Materials Research Bulletin 47 (2012) 1021–1027.